J. Braz. Chem. Soc., Vol. 11, No. 2, 121-128, 2000.
Printed in Brazil

0103 - 5053 $6.00+0.00

Article

Kinetic Analysis of the Chemical Processes in the Decomposition of Gaseous Dielectrics by a Non-Equilibrium Plasma - Part 1: CF_4 and CF_4/O_2 .

Glauco F. Bauerfeldt and Graciela Arbilla*

Departamento de Físico-Química, Instituto de Química, Universidade Federal do Rio de Janeiro,
Sala 408, CT Bloco A, Cidade Universitária, 21949-900, Rio de Janeiro - RJ, Brazil

A integração numérica das equações diferenciais ordinárias que descrevem um sistema cinético e a análise de sensibilidade dos resultados aos parâmetros são metodologias cada vez mais utilizadas na cinética química. Neste trabalho, é apresentado um estudo de simulação numérica da decomposição em fases gasosa de CF_4 e de misturas CF_4/O_2 na presença de silício. É analisada a importância relativa dos processos individuais e são calculados os coeficientes de sensibilidade e o efeito da incerteza nos parâmetros. Os resultados são comparados com dados experimentais da literatura para ajustar os parâmetros do modelo. O principal agente de corrosão neste sistema é o flúor atômico. As concentrações das principais espécies (SiF_4, CO, CO_2 e COF_2) dependem da composição da mistura.

Numerical integration of the coupled differential equations which describe a chemical reacting system and sensitivity analysis are becoming increasingly important tools in chemical kinetics. In this work, a numerical modelling analysis of the chemical processes in the gas-phase decomposition of pure CF_4 and CF_4/O_2 mixtures, in the presence of silicon, was performed. The relative importance of individual processes was analysed and the sensitivity coefficients as well as the effect of the parameters uncertainties were determined . The results were compared with experimental data from the literature to adjust the model parameters. The main etching agent in the system is the fluorine atom. The concentrations of the main species (SiF_4, CO, CO_2 and COF_2) depend on the composition of the mixture.

Keywords: sensitivity analysis, rate of production analysis, CF_4 decomposition

Introduction

Models for the plasma chemistry of SF_6/O_2 and CF_4/O_2 mixtures have been extensively investigated by different research groups[1-18]. The complexity of the involved processes makes it very difficult to develop and solve a complete model to explain and predict experimental results[19,20].

Such models should consider the homogeneous processes in the gas phase and the heterogeneous processes occurring at the gas-solid interface. Some aspects, such as free radical chemistry, electron impact dissociation rates for molecules and radicals, electron number density in the plasma, energy distribution for electrons and chemical species and also the need of solving the system in spatial and temporal coordinates, require an exact approach beyond the capabilities of current computational resources.

In this work, we used the submodel approach which is also frequently applied in other areas of kinetic and numerical modeling such as atmospheric and combustion chemistry[21]. Our main goal was to obtain a good description of the principal chemical processes in the gaseous phase and to analyse the relative importance of individual reactions and the parameters influence in the model results by estimating the sensitivity coefficients S_{ij} for the species (i) towards the parameters of the model (λ_j). Thus, we constructed chemical submodels in which the other processes are considered in a parameterised, simplified way. The present submodels use a semi-empirical approach in which phenomenological dissociation rates, calculated from the measured conversions of the feed gases in experimental studies, are incorporated and where the analysis is centered on the description of the neutral gas-phase chemistry which occurs in the plasma as the ionic species analysis did not prove relevant[18].

Formulation of the models

The models of Edelson and Flamm[3] and Ryan and Plumb[4,5] were used as a basis for the present kinetic scheme. The complete set was introduced and discussed by Bauerfeldt and

---

*e-mail: graciela@iq.ufrj.br

Arbilla[18] in a previous work on the plasma etching of silicon. This set of reactions included surface phenomena as physical adsorption and desorption, as well as surface reactions. The plasma was considered a source of ions and electrons which led to CF_4 dissociation and to atomic fluorine production.

Experimental data from Smolinsky and Flamm[22], were also used to choose the boundary conditions, the parameters of the model and to test the validity of the model results. In that work, the CF_4/O_2 mixtures at a total gas number density of 1.6×10^{16} cm^{-3} (0.5 Torr) flowing in a 5 cm length aluminum tube, were excited by a 49 W, 13.56 MHz discharge. The stable products analysis was performed up to 10 cm downstream from where the discharge started.

The most uncertain aspects in the formulation of this submodel are the electron impact dissociation rate for CF_4, the rate constants for gas-phase free radical reactions and the heterogeneous processes. Electron impact dissociation rates can be calculated from estimated electron number density, electron energy distribution and electron impact dissociation cross-section of the interest species. Plumb and Ryan[4] have made such estimates which are expected to be accurate within one order of magnitude. From measured results[22,23] the dissociation coefficients for CF_4 and O_2 can be estimated in the experimental conditions. In our model, these values were adjusted as parameters in order to fit the experimental dissociation rates.

For the boundary conditions of our work, a plug flow in a cylindrical tube was assumed. The plasma region of the reactor corresponds to a gas mixture residence time of 2.25×10^{-2} s. The space beyond the plasma region, called afterglow, was also included in the calculations, what leads to a total residence time in the reactor of 4.45×10^{-2} s. The adsorption of gas phase species on the reactor wall and further reaction or desorption to return to the gas phase were considered in a simplified way.

The numerical method

The set of differential equations were solved using the fourth order Runge-Kutta-Semi-Implicit Method[24] as implemented in the package KINAL[25]. The relative relevance of each reaction was first evaluated by calculating the contribution of each step to the total rate of concentration change for each species. Then, in order to evaluate the effect of parameters uncertainties on the predicted concentrations, the sensitivity coefficients[26] were calculated by the Direct Decomposed Method[27]. In addition to the relevance and sensitivity analysis, another test was done by changing some of the parameters within their range of uncertainties. This calculation was necessary as some of the parameters and constants are quite hard to evaluate, such as electron number density, branching ratios and heterogeneous reaction rate coefficients.

Results and Discussion

As described above, the reaction set used for the sensitivity calculations was previously employed to describe the plasma etching of silicon by pure CF_4 and CF_4/O_2 mixtures, and can be found in our previous paper[18]. This reaction set was proposed to fit experimental data from Smolinsky and Flamm[22]. Initial conditions for the simulation are listed in Table 1 and are the same as used in reference 18.

Table 1. Numerical simulations initial conditions.

Temperature	313K
Total pressure	0.5 Torr
Flow	24.37 cm^3STP/min
Plasma length	5.0 cm
Initial Concentrations (molecules cm^{-3})	
Total [M]	1.54×10^{16}
$[CF_3]$	1.00×10^{10}
[F]	1.00×10^{10}
[Si]	1.00×10^{14}
$[CF_{3(s)}]$	1.00×10^{10}

Pure CF_4

There is no direct experimental evidence about the branching ratio for CF_4 decomposition. Some indirect information may be obtained from CF_4/O_2 results, as will be discussed below. Clearly, this ratio is an important parameter of the model. In this work we explored the effect of a wide range of values. Following electron impact, CF_4 may dissociate to CF_3 and CF_2 radicals. In fact these are probably non direct processes. The direct dissociation of CF_4 through the reaction:

$$e^- + CF_4 \rightarrow CF_3 + F + e^- \tag{1}$$

proceeds only at high electron energies (12.5 eV threshold)[28]. More recent data[29] show that the alternative reaction:

$$e^- + CF_4 \rightarrow CF_3 + F^- \tag{2}$$

is relatively faster and proceeds at lower energies, 5 - 6 eV. This reaction is followed by the rapid detachment reaction:

$$e^- + F^- \rightarrow 2e^- + F \tag{3}$$

This sequence being equivalent to reaction 1.

In a similar way, it was proposed[30] that CF_2 is produced through the rapid dissociation of an excited state of CF_3 radical which in turn is formed from CF_4 decomposition. In the time scale of the experiments, the CF_2 production may be considered a direct process after electron impact of CF_4:

$$e^- + CF_4 \rightarrow CF_2 + 2F + e^- \tag{4}$$

Branching ratios $k_{CF4 \rightarrow CF2} / k_{CF4 \rightarrow CF3}$, k_j being the rate constant for the reaction j, from 14 to zero were tested.

The best results, when compared with experimental data, are obtained when the primary dissociation of CF_4 favours the formation of CF_2 by a factor 2.3. Because of that a ratio of 2.4, as estimated by Plumb and Ryan[4], was used.

Table 2 shows the relative importance of individual reactions, based on a rate of production analysis, for the main gaseous species. The production of CF_2 by electron impact of CF_3 is a negligible path of reaction for CF_3 radicals. Reactions of CF_3 with neutral species F and F_2 are the main path of consumption of the radical. Also, at the early stages of reaction, when F and F_2 concentrations are still low, the recombination to C_2F_6 appears an important path.

Our simulations show that the rate of the recombination processes is at least 10^3 times faster than the electron impact dissociation, not included in the final model. Also, since CF_4 concentration is 10^2 - 10^3 times greater than CF_3 concentration, the direct electron dissociation of CF_3 radical is a negligible source of CF_2 when compared with CF_4 dissociation to produce $CF_2 + 2$ F. A similar situation arises for CF_2 radicals. The electron impact dissociation, to give CF + F, is at least 30 times slower than the recombination reaction of CF_2 with F atoms. Also, CF_2 dissociation is a negligible source of F atoms when compared with the primary CF_4 dissociation to produce $CF_2 + 2$ F.

CF_3 and CF_2 dissociation processes may be included in a more comprehensive reaction set, in order to obtain a better description of the system. Nevertheless, it would not lead to important changes in the results of the model mainly due to the uncertainties in primary dissociation rates and heterogeneous reactions of atoms.

The plasma chemistry is highly influenced by the dissociation and recombination processes of CF_2 and CF_3 . Clearly, the main recombination reaction of CF_3 is with F atom. This fast reaction controls the CF_3 concentration and restricts the amount of CF_4 consumed to very low values. At the end of the discharge region (5 cm) 96% of the initial CF_4 remains. In the afterglow region, where electron dissociation ceases, the reforming of CF_4, through reactions

$$CF_3 + F + M \rightarrow CF_4 + M \qquad (5)$$

$$CF_3 + F_2 \rightarrow CF_4 + F \qquad (6)$$

continues and, because of that, a net consumption of 2 % is found at 10 cm.

Table 2. Contribution of individual reactions to kinetic processes in the plasma region.

Process	**Rate (particles cm^{-3} s^{-1})**		
	Pure CF_4	**25% O_2 / 75% CF_4**	**80% O_2 / 20% CF_4**
Main reactions for CF_2 radicals			
$CF_2 + F \rightarrow CF_3$	-3.183×10^{16}	-4.052×10^{14}	-4.963×10^{12}
$CF_2 + O(^3P) \rightarrow COF + F$	zero	-2.016×10^{16}	-5.416×10^{15}
$CF_2 + O(^3P) \rightarrow CO + 2F$	zero	-5.760×10^{15}	-1.547×10^{17}
$CF_2 + COF \rightarrow CO + CF_3$	zero	-3.695×10^{11}	-1.191×10^{9}
$CF_2 + COF \rightarrow CF + COF_2$	zero	-3.695×10^{11}	-1.191×10^{9}
Main reactions for CF_3 radicals			
$CF_3 + F + M \rightarrow CF4 + M$	-3.904×10^{16}	-1.198×10^{15}	-1.591×10^{13}
$2 CF_3 \rightarrow C_2F_6*$	-7.665×10^{15}	-4.752×10^{11}	-1.7181×10^{9}
$CF_3 + F_2 \rightarrow CF_4 + F$	-2.142×10^{15}	-1.669×10^{14}	-1.022×10^{12}
$CF_3 + F^- \rightarrow e^- + CF_4$	-5.641×10^{2}	-1.753×10^{2}	-1.109×10^{0}
$CF_3 + O(^3P) \rightarrow COF_2 + F$	zero	-9.794×10^{15}	-2.853×10^{15}
$CF_3 + O2 + M \rightarrow CF_3O_2 + M$	zero	-1.970×10^{14}	-3.782×10^{13}
$CF_3 + COF \rightarrow CO + CF_4$	zero	-2.703×10^{12}	-9.441×10^{9}
$CF_3 + COF \rightarrow CF_2 + COF_2$	zero	-2.703×10^{12}	-9.441×10^{9}
$CF_3 \rightarrow CF_3(s)$	-8.295×10^{14}	-6.531×10^{12}	-3.927×10^{11}
$CF_3 + CF_3(s) \rightarrow C_2F_6(s)$	-9.308×10^{11}	-1.612×10^{8}	-1.233×10^{6}
Main reactions for F atoms			
$CF_3 + F + M \rightarrow CF_4 + M$	-3.904×10^{16}	-1.198×10^{15}	-1.591×10^{13}
$2F + M \rightarrow F_2 + M$	-4.791×10^{15}	-1.099×10^{17}	-5.362×10^{15}
$CF2 + F \rightarrow CF_3$	-3.183×10^{16}	-4.052×10^{14}	-4.963×10^{12}
$F + COF + M \rightarrow COF_2 + M$	zero	-1.152×10^{15}	-1.479×10^{13}
$F + CO + M \rightarrow COF + M$	zero	-1.564×10^{14}	-9.228×10^{12}
$F + O_2 + M \rightarrow FO_2 + M$	zero	-5.052×10^{14}	-3.563×10^{14}
$F + FO_2 \rightarrow F_2 + O2$	zero	-2.087×10^{14}	-1.107×10^{13}
$F \rightarrow F(s)$	-8.852×10^{15}	-3.450×10^{16}	-7.620×10^{15}
$F + CF_3(s) \rightarrow CF4(s)$	-9.929×10^{13}	-8.512×10^{12}	-2.390×10^{11}
$F + Si \rightarrow SiF/Si$	-2.526×10^{5}	-6.350×10^{14}	-3.949×10^{15}
$F + SiF/Si \rightarrow SiF_2/Si$	-2.526×10^{15}	-6.351×10^{14}	-3.949×10^{15}
$F + SiF_2/Si \rightarrow SiF_3/Si$	-2.526×10^{15}	-6.351×10^{14}	-3.949×10^{15}
$F + SiF_3/Si \rightarrow SiF_4/Si$	-2.526×10^{15}	-6.351×10^{14}	-3.949×10^{15}

Figures 1 and 2 show the first-order local concentration sensitivity coefficients S_{ij} for the main species towards the parameters of the model. As usual, these coefficients, elements of the local concentration sensitivity matrix, are defined as

$$S_{ij} = \partial Y_i / \partial \lambda_j$$

were Y_i are the concentrations of the chemical species and λ_j are the parameters of the model. The sensitivity matrix, **S**, represents a linear approximation of the dependence of the solutions on parameters changes. The change of a parameter belonging to reaction *j* causes a direct concentration change in those species which are reactants or products in that reaction. Also, the direct concentration changes cause further differences in the concentration of other species. The latter, indirect, effects are non-linear and can not be predicted by screening analysis[25b]. This non-linear effects can be revealed by sensitivity analysis. The information taken from these coefficients is rather different from that taken from the so-called brute force method, where a parameter (for example the electron density) is changed. The S_{ij} values are local, since they belong to a time interval defined by the time of the perturbation t_1 and the time of the observation t_2 and, also, they represent the perturbation on a species *i*, while all the others are kept constant. On the other hand, the previous analysis showed the effect of a substantial change on one of the parameters, during the total time of observation t_2[25b]. The information taken from all the analysis done here is complementary and should be considered as a whole in order to assess the relevance and interconnection of parameters and variables and to decide whether a reaction or a chemical species may be eliminated from the model, or not.

The high level of CF_2 concentration relative to CF_3 is due to two factors: as shown in Figures 1 and 2, CF_2 formation through the reaction $e^- + CF_4 \rightarrow CF_2 + 2F + e^-$ is faster than CF_3 production reactions1 and

$$F + CF_2 \rightarrow CF_3 \qquad (7)$$

by a factor of about 1.5. Also, the rate of consumption of CF_3 by reaction 5 is about 1.2 times greater than that for CF_2 recombination reaction 7.

In the plasma region stable C_2F_6 grows steadily. CF_3 recombination reaction to produce the vibrationally excited species $C_2F_6{}^*$:

$$2\ CF_3 \rightarrow C_2F_6{}^* \qquad (8)$$

takes account of about 15.5% of the total lost of CF_3 radicals. The model considers the C_2F_6 electron dissociation:

$$e^- + C_2F_6 \rightarrow 2\ CF_3 + e^- \qquad (9)$$

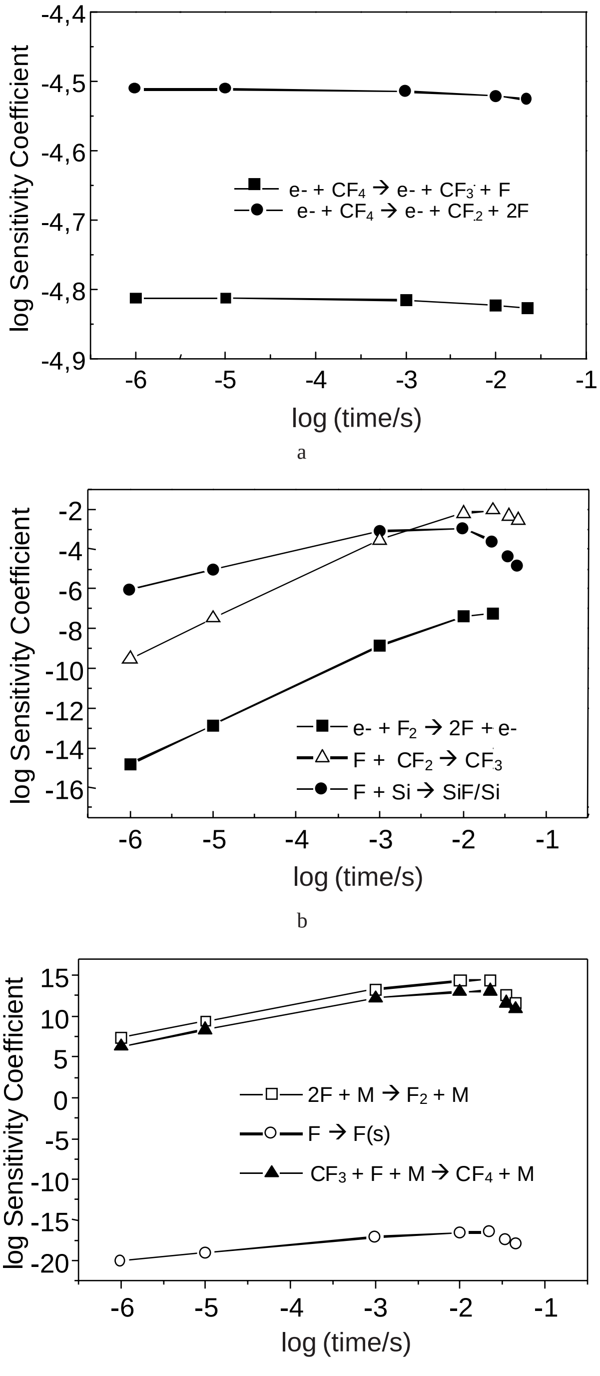

a

b

c

Figure 1. Sensitivity coefficients for atomic fluorine reactions for the plasma etching of silicon in pure CF_4 as a function of time.

The dissociation coefficient used by Edelson and Flamm[3] leads to a considerable reduction of C_2F_6 concentration, since the rate of C_2F_6 electron dissociation is about 0.5 times the rate of C_2F_6 production by CF_3 radical recombination. If the rate coefficient of Ryan and Plumb[4,5], 20 times smaller, is used, the contribution of C_2F_6 electron dissociation reaction drops to virtually zero and C_2F_6

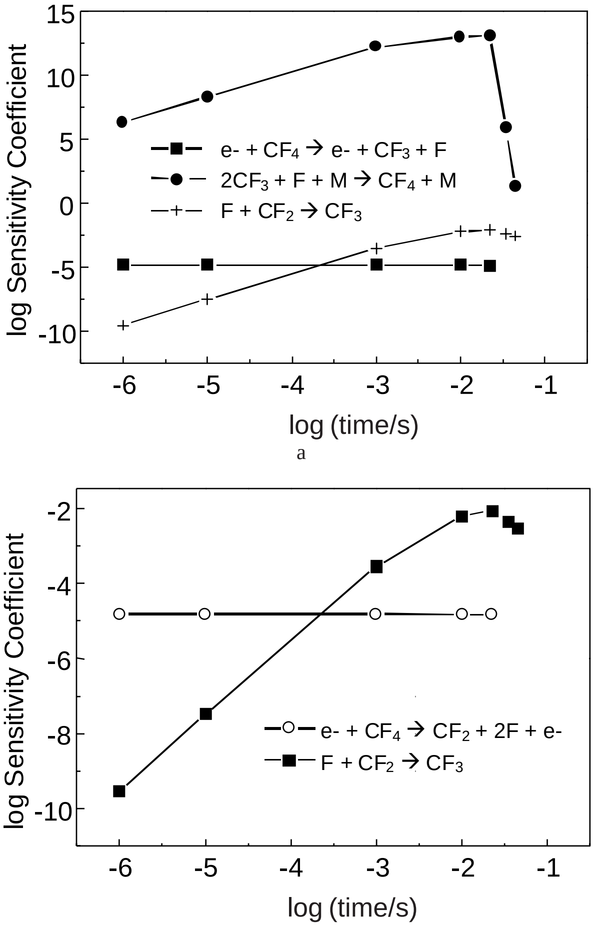

a

b

Figure 2. Sensitivity coefficients for CF_3 (2a) and CF_2 reactions (2b) for the plasma etching of silicon in pure CF_4 as a function of time.

concentration increases by a factor of 2. Nevertheless, CF_3 concentration does not alter significantly since that electron dissociation contributes in about 6% to its formation.

In the post-discharge region CF_3 concentration drops drastically and very little C_2F_6 is further formed. In this region, the main recombination reactions are with F and F_2. Also, in this region a considerable fall of CF_2 concentration occurs, mainly because the production of CF_2 by CF_4 electron dissociation stops and the rapid recombination reaction with F atoms continues downstream.

The silicon etching process was modelled as a sequence of single F atom reactions which forms SiF_4 on the surface (SiF_4/Si) that subsequently desorbs to the gas phase. The choice of atomic fluorine as the active etching is supported in previous experimental and simulated data[1-20]. As in the previous works[3,5] the first F atom reaction was chosen as the limiting step in order to emulate experimental results[31]. Silicon was assumed to be uniformly distributed in the reactor. In the presence of Si, the F atom concentration is reduced in about 10-15% for a silicon number density of 1×10^{14} particles cm^{-3} and in about 25% for a silicon number density of 1.6×10^{16} particles cm^{-3} . The value of the rate coefficient for:

$$F + Si \rightarrow SiF/Si \tag{10}$$

is certainly one of the most uncertain aspects in the formulation of the model. In this work we used the value of Edelson and Flamm[3] and also the value of Ryan and Plumb[5], which is smaller by a factor of 4.6. The results for SiF_4, CF_3, CF_2 and F differ in less than 25% which is not a significant figure when considering the other uncertainties of the model.

Another uncertain parameter of the model is the electron number density in the plasma. The main sources of F atoms are reaction 1 and 4 which depend on electron number density. The values of Edelson and Flamm[3] (1×10^{10} cm^{-3}) and Ryan and Plumb[5] (6×10^{10} cm^{-3}) were both tested. The best agreement with experimental results[22] is obtained for an electron number density of 1.0×10^{10} cm^{-3} , a silicon number density of 1.0×10^{14} cm^{-3} and with a rate constant of 4.61×10^{-13} $molec^{-1}$ cm^3 s^{-1} for reaction 9.

The results stress our previous conclusions: the shape of the sensitivity curves follows the general shape of the individual rate curves[18] and the ratio between the S_{ij} values is closely related to the contribution of each reaction (Table 2). For example, $S_{F,\, CF4 \rightarrow CF2}$[32] values are twice the $S_{F,\, CF4 \rightarrow CF3}$ values and are nearly constant within the plasma region (Figure 1a). The $S_{F,\, j}$ values for the atomic fluorine association reactions with CF_2 and Si (Figure 1b) show that for small residence times, the changes in F + Si association rate constant will affect F concentrations more than the changes in F + CF_2 association rate constant. The inverse holds for longer residence times. That is a direct consequence of the contribution of F + Si association, on the silicon surface, being more important at the reactor entrance or for short times and the contribution of F + CF_2 association being more important as the CF_2 concentration grows up. Also, the S_{Fj} coefficients (Figures 1b and 1c) show that the more relevant reactions for atomic fluorine are the production reactions CF_3 + F and CF_2 + F and the recombination to form F_2.

Similar results were obtained for CF_2 and CF_3 sensitivity coefficients. The values for $S_{CF3,\, CF3 + F + M \rightarrow CF4 + M}$ /[M] and $S_{CF3,\, F + CF2 \rightarrow CF3}$ are similar, except in the post discharge region, where changes in F + CF_2 association rate constant should affect more the CF_3 concentration (Figure 2a). For CF_2 radicals, Figure 2b, the system is more sensitive to changes in F + CF_2 association rate constant. Because of the non linearity of the system, a perturbation in CF_4 electron dissociation rate to give CF_2 + 2F leads to a rather small change in [CF_2] , which recombines, further, with fluorine atoms. In other words, since CF_2 production from CF_4 and consumption by association with atomic fluorine reactions are coupled, small changes in the former hardly affect the radical concentration.

CF_4 / O_2 Mixtures

In our previous work on the plasma etching of silicon by CF_4/O_2 mixtures, F, CF_3 and CF_2 concentrations dependence on the oxygen concentration was suggested, both in the plasma region and in the afterglow region[18].

In the presence of oxygen, the O atoms, which are mainly formed through electron impact dissociation of the molecule:

$$e^- + O_2 \rightarrow 2\,O(^3P) + e^- \tag{11}$$

and

$$e^- + O_2 \rightarrow O(^3P) + O(^1D) + e^- \tag{12}$$

compete with F atom for CF_3 and CF_2 radicals through reactions:

$$CF_3 + O(^3P) \rightarrow COF_2 + F \tag{13}$$

$$CF_2 + O(^3P) \rightarrow COF + F \tag{14}$$

$$CF_2 + O(^3P) \rightarrow CO + 2F \tag{15}$$

The rate constant of $CF_2 + O(^3P)$ reaction is one order of magnitude higher than the rate constant for the F + CF_2 recombination. For the set of rate constants used in this model, the reverse situation holds for CF_3 .

Thus, in the presence of O_2 , new intermediates and new products (COF, COF_2, CO and CO_2) appear[18] and also the concentration of F, CF_2 and CF_3 are controlled by the coupled association and recombination reactions of CF_2 and CF_3 with either F or $O(^3P)$. The relative relevance of reactions with F and O atoms changes with the composition of the mixture. For low concentrations of O_2, the reactions of CF_2 and CF_3 with F atoms become relevant and a significant fraction of COF is converted to COF_2. At high concentrations of O_2, COF is almost completely oxidised to CO_2 . The ratio (3.5) between the $O(^3P)$ reaction with CF_3 and CF_2 rate constants is slightly higher than the ratio (2.5) between CO_2 and CO concentrations, showing that part of COF is still reacting with F.

Table 2 compares the rate of sink reactions for F, CF_2 and CF_3. The entries of the table show some of the significant differences between the results for pure and oxygenated mixtures. With low concentrations of molecular oxygen, a very significant fraction of CF_2 is still converted to CF_3 through association with atomic fluorine. The COF which is formed by reaction of O atoms with CF_2 , reacts further with atomic fluorine to produce COF_2 . Only a minor part of COF reacts with oxygen producing CO_2 .

At high relative concentrations of molecular oxygen in the feed gas, the CF_2 produced in the primary dissociation step reacts exclusively with O atoms forming CO and COF which are rapidly converted to CO_2. In the same way, the CF_3 is converted rapidly to COF_2, which may dissociate to COF and ultimately CO_2 and CO.

Some of the sensitivity coefficients are presented in Figures 3 and 4. The sensitivity coefficients for the formation reactions (Figures 3a, 3b and 3c) follow the relative importance of individual reactions, that is $S_{F,CF4 \rightarrow CF2\,+\,2F} > S_{F,CF4 \rightarrow CF3\,+\,F}/[M] > S_{F,F2 \rightarrow 2F}/[M]$. Also, these $S_{F,j}$ values are higher than values for reactions 13 – 15 (Figure 3c). The $S_{F,j}$ coefficients calculated for the main sink reactions (Figures 3a, 3b and 3c), in the presence of O_2, show that in that environment the main atomic fluorine reaction is the self recombination to form F_2, as confirmed by Table 2.

The $S_{F,j}$ coefficients calculated for reactions

$$COF + O(^3P) \rightarrow CO_2 + F \tag{16}$$

and

$$COF + F + M \rightarrow COF_2 + M \tag{17}$$

follow the same trend, the ratio between them being approximately the [M] value (Figure 3d). For the 75% CF_4 / 25% O_2 mixture, the $S_{F,COF+O(3P) \rightarrow CO2+F}$ value is about 15 times the $S_{F,COF+F \rightarrow COF2}/[M]$ since the COF , which is formed by reaction of O atoms with CF_2, reacts with O to produce CO_2, rather than with F, to produce COF_2. For these plasmas where the CF_4/O_2 ratio in the feed gas is higher, the $S_{F,COF+F \rightarrow COF2}/[M]$ becomes relatively higher.

The sensitivity coefficients for COF_2 (Figure 4a) and COF (Figure 4b) confirm that the main path of formation of COF_2 is the reaction between CF_3 and $O(^3P)$ atoms, which is about 27 times faster than reaction 17 (COF + F + M à COF_2 + M). Finally, in the plasma region, reaction between CF_2 and $O(^3P)$ to form COF:

$$CF_2 + O(^3P) \rightarrow COF + F \tag{18}$$

is about 16 times faster than the further reaction of COF with atomic fluorine (reaction 16). This result is also shown by the comparison of the sensitivity coefficients $S_{COF,COF+F \rightarrow COF2}/[M]$ and $S_{COF,CF2+O(3P) \rightarrow COF+F}$ (Figure 4b). Downstream of the discharge region, atomic oxygen concentration dramatically drops through reactions with CF_2 and COF and the formation of the final product COF_2 predominates.

In Figure 5 the rate of formation of gaseous SiF_4 as function of the distance from the origin and the mole percent of O_2 in the feed is displayed. Since in this model atomic fluorine is the active etching agent and the primary etching reaction was considered rate controlling, the surface in Figure 5 closely reproduces the change in atomic fluorine concentration with distance from the origin and the mole percent of O_2 in the feed[18].

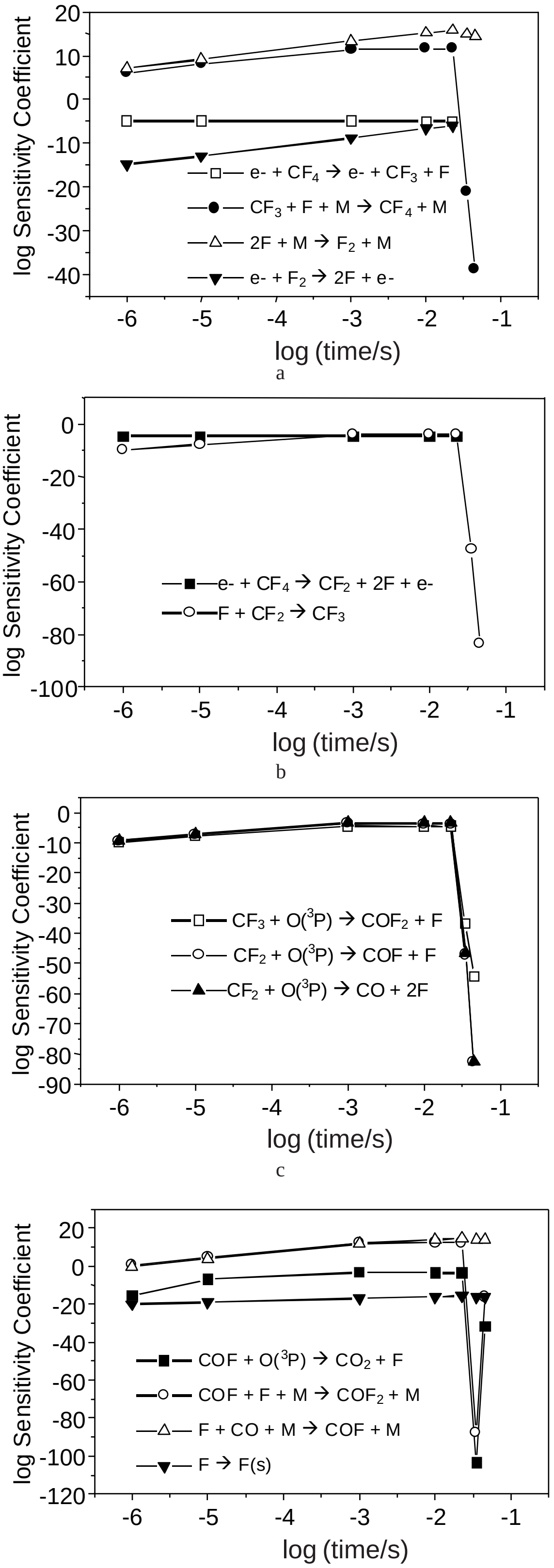

Figure 3. Sensitivity coefficients for atomic fluorine reactions for the plasma etching of silicon in a mixture 75% CF_4 and 25% O_2 as a function of time.

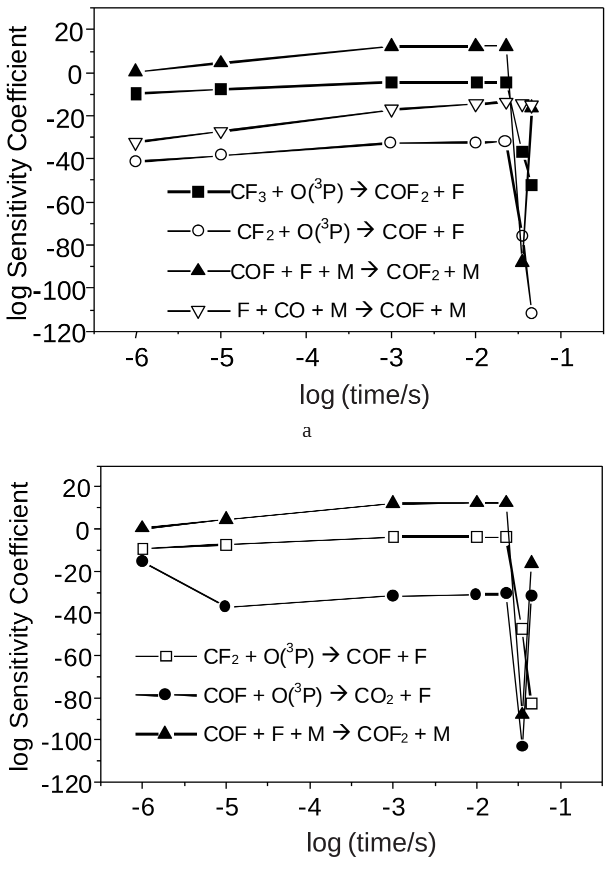

Figure 4. Sensitivity coefficients for COF_2 (4a) and COF (4b) reactions for the plasma etching of silicon in a mixture 75% CF_4 and 25% O_2 as a function of time.

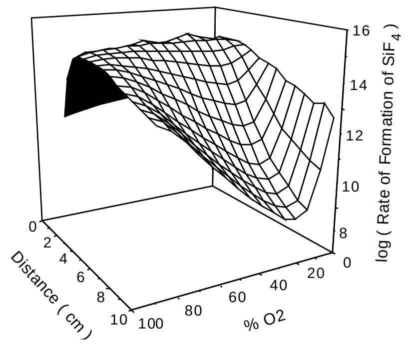

Figure 5. Rate of formation of gaseous SiF_4 as a function of the distance from the discharge origin and the mole percent of O_2 in the feed.

Conclusions

The main goal of this work was to analyse the chemical processes in the plasma decomposition of CF_4 and CF_4/O_2 mixtures in the presence of silicon. The rate of production and sensitivity analysis, as well as the computed concentrations, show that the major features of plasma etching of silicon are explained in terms of gas-phase reactions. For this system, positive and negative ionic species were also considered, and incorporated to the model using literature experimental rate coefficients. The results showed that reactions involving these species are not important in determining the gas phase chemistry.

The model reproduces the experimental conclusion that atomic fluorine is the active etching agent. The fact that the primary etching reaction appears to be the most significant process and the sequential fluorination reactions have no significant sensitivities, is due to the fact that their rates were purposely chosen not to be rate-controlling.

For a complex system with significant uncertainties, such as this, the more important contribution of modelling is to demonstrate, through the rate of production and the sensitivity analysis, which reactions require further experimental or theoretical investigation.

The importance analysis shows that many key processes are poorly known and need a better determination. The major uncertainties in the gas phase chemistry are the branching ratios for the primary dissociation processes, the cross sections for electron impact dissociation and the electron number densities.

The extension of these chemical sub-models to more complete models will involve a better determination of the surface chemistry and the transport of radicals and ions, which were crudely parameterised in this work. The formulation of a complete model must also involve the consideration of the energy distribution of particles and temperature gradients. These results may be considered as an extension of previous chemical models and provide forward insight into the chemical processes details.

Acknowledgements

The authors thank partial financial support from CNPq and FAPERJ. They also thank Prof. T. Turányi (Central Research Institute of Chemistry, Budapest, Hungary) for a free copy of KINAL package and Prof. Gerardo Gerson B. de Souza (DFQ/IQ/UFRJ) for his interest in this project.

References

1. Mogab, C. J.; Adams, A. C.; Flamm, D. L. *J. Appl. Phys*. **1976**, *49* , 3796.
2. Kushner, M. J. *J. Appl. Phys*. **1982**, *53* , 2923.
3. Edelson, D.; Flamm, D. L. *J. Appl. Phys*. **1984**, *56*, 1522.
4. Plumb, I. C.; Ryan, K. R. *Plasma Chem. Plasma Process*. **1986**, *6* , 205.
5. Ryan, K. R.; Plumb, I. C. *Plasma Chem. Plasma Process*. **1986**, *6* , 233.
6. Plumb, I. C.; Ryan, K. R. *Plasma Chem. Plasma Process*. **1986**, *6* , 247.
7. Kline, L.E. *IEEE Trans. Plasma Sci.* **1986,** *PS-14* , 145.
8. Anderson, H. M.; Merson, J. A.; Light, R. W. *IEEE Trans. Plasma Sci.* **1986**, *PS-14*, 156.
9. Venkatesan, S. P.; Trachtenberg, I.; Edgard, T. F. *J. Electrochem. Soc*. **1987**, *134* , 3194.
10. Ryan, K. R. *Plasma Chem. Plasma Process.* **1989**, *9*, 483.
11. Economou, D. J.; Park, S. K.; Williams, G. *J. Electrochem. Soc.* **1987**, *134* , 3194.
12. Venkatesan, S. P.; Edgard, T. F.; Trachtenberg, I. *J. Electrochem. Soc.* **1989**, *136* , 536.
13. Ryan, K. R.; Plumb, I. C. *Plasma Chem. Plasma Process.* **1990**, *10* , 207.
14. Lii, Y. J.; Jorné, J.; Cadien, K. C.; Schoenholtz Jr., J. E. *J. Electrochem. Soc*. **1990** , *137* , 3633.
15. Park, S. K.; Economou, D. J. *J. Electrochem. Soc.* **1991**, *138* , 1499.
16. Kopalidis, P. M.; Jorné, J. *J. Electrochem. Soc.* **1993**, *140* , 3037.
17. Khairallah, Y.; Khonsari-Arefi, F.; Amouroux, J. *Pure Appl. Chem.* **1994**, *66* , 1353.
18. Bauerfeldt, G. F.; Arbilla, G. *Quím. Nova* **1998**, *21*, 25.
19. Manos, D. M.; Flamm, D. L. *Plasma Etching: An Introduction*; Academic Press; San Diego, CA , 1989.
20. Ryan, K.R.; Plumb, I.C.; *Crit. Rev. Solid State Mater. Sci*. **1988**, *15* , 153.
21. Finlayson-Pitts, B. J.; Pitts Jr., J. S. *Atmospheric Chemistry: Fundamentals and Experimental Techniques*; John Willey & Sons ; New York, 1986.
22. Smolinsky, G.; Flamm, D. L. *J. Appl. Phys*. **1979**, *50*, 4982.
23. d'Agostino, R.; Flamm, D. L. *J. Appl. Phys.* **1981**, *52*, 162.
24. Kaps, P.; Rentrop, P. *Numer. Math*. **1979** , *33*, 55.
25. (a) Turányi, T. *Comput. Chem*. **1990**, *14*, 3, 253. (b) Turányi, T. *J. Math. Chem*. **1990**, *5*, 203.
26. (a) Steinfeld, J. I.; Francisco, J. S.; Hase, W. L. *Chemical Kinetics and Dynamics*; Prentice Hall, Englewood Cliffs; New Jersey, 1989. (b) Pilling, M. J.; Smith, I. W. M. *Modern Gas Kinetics. Theory, Experiment and Application* Blackwell Scientific Publications; Oxford, 1987. (c) Hirst, D. M. *A Computational Aproach to Chemistry*; Blackwell Scientific Publications; Oxford, 1990.
27. Valkó, P.; Vajda, S. *Comput. Chem*. **1984**, *8*, 255.
28. Winters, H. F.; Inokuti, M. *Phys. Rev.* **1982**, *A25*, 1420.
29. Hunter, S. R.; Christophorou, L. G. *J. Chem. Phys*. **1984**, *80* , 6150.
30. Flamm, D. L. *J. Appl. Phys*. **1980**, *51*, 5688.
31. Flamm, D. L. Donnelly, V. M. *Plasma Chem. Plasma Process.* **1981**, *1*, 317.
32. In this work, the symbol $S_{F,CF4 \rightarrow CF2}$ is used to indicate the sensitivity coefficient of species i = F towards the rate constant for reaction e- + $CF_4 \rightarrow CF_2$ + 2F + e-. A similar nomenclature is used for the other S_{ij} coefficients.

Received: September 22,1998